DOI: 10.55415/deep-2023-0016.v1

Discovery of a Pyridophenoselenazinium-based Photosensitizer with High Photodynamic Efficacy against Breast Cancer Cells

Guiling Li[b#], Peixia Li [a#], Qiaoyun Jiang [a], Qianqian Zhang [a], Jingru Qiu[a], Donghai Li[b] *, Gang Shan[a]*

[a]Department of Medicinal Chemistry, Key Laboratory of Chemical Biology (Ministry of Education), School of Pharmaceutical Sciences, Cheeloo College of Medicine, Shandong University, 44 Wenhuaxi Road, Jinan, Shandong Province 250012, P. R. China.

[b]Advanced Medical Research Institute, Meili Lake Translational Research Park, Cheeloo College of Medicine, Shandong University, Jinan, Shandong, 250012, P. R. China.

[#]These authors contributed equally to this work.

*Corresponding authors:

Prof. Dr. Gang Shan. E-mail: gangshan@sdu.edu.cn

Prof. Dr. Donghai Li. E-mail: lidonghai@sdu.edu.cn

Key words: Photodynamic therapy, Photosensitizer, Pyridophenoselenazinium dye, Breast cancer

DOI: 10.55415/deep-2023-0016.v1

ABSTRACT

Development of efficient photosensitizers with minimal side effects is highly desirable in photodynamic therapy. Reported herein is the discovery of a novel pyridophenoselenazinium-based NIR-I photosensitizer, termed **PPSe**, that can efficiently generate both type I and type II reactive oxygen species (ROS) upon appropriate light irradiation. **PPSe** exhibited potent phototoxicity as well as excellent phototherapeutic indexes against several breast cancer cell lines. It was demonstrated that **PPSe** could induce DNA damage and breast cancer cell apoptosis via photo-triggered intracellular ROS generation.

DOI: 10.55415/deep-2023-0016.v1

1. INTRODUCTION

Breast cancer (BC) is the most common cancer among women, and one of the leading causes of female morbidity and mortality, with 2.26 million new cases and 680,000 deaths in 2020 all over the world [1-3]. Thus, breast cancer remains a major public health burden. Current breast cancer therapies mainly rely on surgery, radiotherapy, chemotherapy, and targeted therapy. However, these strategies are suffering from the issues of physical pain, fatal side effects and drug resistance [4-6]. The situation for aggressive triple negative breast cancer (TNBC) is even worse due to its lack of progesterone receptor (PR), human epidermal growth factor receptor 2 (HER2) and estrogen receptor (ER) [7, 8]. Therefore, it is of great importance to develop more efficient and less toxic therapies for breast cancer treatment, especially TNBC.

In recent years, photodynamic therapy (PDT) has attracted much interest for breast cancer treatment owing to its advantages of low systemic toxicity, minimal invasiveness, negligible drug resistance and cost-effective [9-11]. In a typical process, PDT utilizes a combination of photosensitizer, light and oxygen to destroy cancer cells. An ideal photosensitizer itself should be non-toxic, but possesses great ROS generation capacity upon light irradiation [12]. Photosensitizers are mainly divided into type I and type II based on the ROS generation mechanism. Upon photoirradiation, type I photosensitizer can produce radical reactive oxygen species, such as superoxide anion radical ($O_2^{\bullet -}$) and hydroxyl radical ($OH^{\bullet}$), via an electron transfer process while type II photosensitizer can convert non-toxic molecular oxygen into highly toxic singlet oxygen ($^1O_2$) via an energy transfer photoreaction [13, 14].

DOI: 10.55415/deep-2023-0016.v1

Type I photosensitizers are thought to be more efficient against solid tumors, due to the electron transfer pathway is less O_2-dependent. A number of photosensitizers have been used in clinical applications over the past 30 years, such as porphyrin, chlorin, phthalocyanine and indocyanine green. However, most clinically used photosensitizers belong to type II, which is high O_2-dependent. In addition, current photosensitizers are still suffering from high dark toxicity, limited penetration depth and challenging synthesis [12, 15]. Therefore, development of new photosensitizers with excellent efficacy and minimal side effects for photodynamic cancer therapy, especially type I photosensitizers, is still in high demand.

Methylene blue is an FDA-approved phenothiazinium-based drug for the treatment of methemoglobinemia with an excellent safety profile, which is also proved to be an antitumor photosensitizer. However, its redox-active property makes it have poor intracellular ROS production capacity and limited therapeutic efficacy. In this work, we reported the discovery of a novel pyridophenoselenazinium-based NIR-I photosensitizer **PPSe** derived from methylene blue, that exhibited potent phototoxicity along with excellent phototherapeutic indexes against several breast cancer cell lines, including MDA-MB-231, MDA-MB-468, MCF-7 and 4T1 cells.

2. MATERIALS AND METHODS

2.1 Determination of singlet oxygen quantum yield

1,3-diphenylisobenzofuran (DPBF) was used to evaluate singlet oxygen production. The singlet oxygen generation of **PPSe** was measured in ethanol solutions and methylene blue (MB) was used as a standard. The absorbance of DPBF at 410 nm was

DOI: 10.55415/deep-2023-0016.v1

adjusted to about 1.0, and the absorbance of **PPSe** and methylene blue at 660 nm was adjusted between 0.2 and 0.4. Then the absorption spectrum was measured after light irradiation (660 nm, 2 mW·cm^{-2}) for 0, 10, 20, 30, 40, 50, 60, 70 and 80 s respectively. The DPBF alone solution was used as control. And the singlet oxygen quantum yield was monitored by measuring the reduction in the absorbance intensity of DPBF at 410 nm using a microplate reader (TECAN). The values of singlet oxygen Φ_Δ were calculated by the following equation:

$$\Phi_\Delta = \Phi_{MB} \times (k_{\mathbf{PPSe}} \times F_{MB})/(k_{MB} \times F_{\mathbf{PPSe}})$$

where, Φ_Δ represents the singlet oxygen quantum yield of **PPSe**; Φ_{MB} is the singlet oxygen quantum yield of methylene blue (0.52 in ethanol); k represents the slope of the decrease of the absorbance at 410 nm of DPBF with the addition of irradiation time; F is the correction factor ($F = 1 - 10^{-OD}$). OD represents the absorbance of the solution at 660 nm.

2.2 Superoxide anion radical ($O_2^{\bullet-}$) detection

To determine the $O_2^{\bullet-}$ generation, dihydrorhodamine 123 (DHR123) was used as a superoxide anion radical probe. **PPSe** was added into DHR123 aqueous solution with the same concentration of 5 μM. And the solutions were exposed to 660 nm irradiation (10 mW/cm^2) for different times. DHR123 without **PPSe** was used as control. The fluorescence intensities of solutions were measured by the spectrofluorometer and the excitation wavelength was 500 nm.

2.3 Cell incubation

DOI: 10.55415/deep-2023-0016.v1

Human breast cancer MDA-MB-231, MCF-7, MDA-MB-468, MDA-MB-453 cells, and mouse breast cancer 4T1 cells were obtained from Shandong University (Jinan, China). The human breast cancer MDA-MB-231, MCF-7, MDA-MB-468, MDA-MB-453 cells were cultured in Dulbecco's Modified Eagle Medium (DMEM) containing 10% fetal bovine serum (FBS) and 1% double antibiotics penicillin/streptomycin (Gibco), and the mouse breast cancer 4T1 cell was cultured in RPMI-1640 cell medium supplemented with 10% FBS and 1% double antibiotics penicillin−streptomycin. All the cells were incubated in a humidified 37°C, 5% CO_2 incubator.

2.4 Cellular uptake

Cellular uptake efficiency of **PPSe** was taken using CytoFLEX S Flow Cytometry (Beckman, USA). 4T1 cells were incubated with **PPSe** (5 μM) for various time points (30 min, 1 h, 3 h, 6 h and 9 h). Then the cells were harvested and re-suspended with phosphate buffer solution and finally analyzed via flow cytometry. The excitation wavelength was 638 nm and the emission collection wavelength of 712 ± 25 nm.

2.5 Intracellular ROS generation

2′,7′-dichlorofluorescein diacetate (DCFH-DA) was used as a probe to assess the *in vitro* ROS generation of **PPSe** in 4T1 cells. The 4T1 cells were incubated with **PPSe** (0.25 μM) for 2 h at 37°C and then co-incubated with DCFH-DA (10 μM, λex = 488 nm, λem = 525 nm) for 30 min at 37 °C in the dark. 4T1 cells were washed after incubation, followed by irradiation (660 nm, 20 mW/cm^2, 10 min). The cells were

DOI: 10.55415/deep-2023-0016.v1

carefully collected and analyzed immediately using flow cytometry (Beckman, USA). Cells in the medium without compound were used as controls, and the experiments were repeated three times.

2.6 Cytotoxicity test

The cytotoxicity of **PPSe** was carried out using the Cell Counting Kit-8 (CCK-8) assay. MDA-MB-231, MCF-7, MDA-MB-468, MDA-MB-453 and 4T1 cells were seeded on a 96-well plate at a density of 5000 cells/ well for 24 h incubation. The photosensitizer **PPSe** was diluted into different concentrations with medium. And the cells were incubated with different concentrations of **PPSe** for 6 hours and then irradiated with 660 nm LED lamp (20 mW/cm^2, 10 min). After 24 h incubation, the CCK-8 stop solution (10 μL) was added to each well and the cell viabilities were measured. Meanwhile, the same concentrations of **PPSe** were added into cancer cells for 24 h in darkness to evaluate the dark cytotoxicity. After CCK-8 treatment, the absorbance at 450 nm of each well was measured by a microplate reader (TECAN) and IC_{50} values were calculated accordingly. The experiments were repeated three times. Cell viability rates (%) and IC_{50} values were analyzed by GraphPad Prism 9.0.7.

2.7 Calcein AM/PI assay

Calcein-AM and propidium iodide (PI) were used to study live/dead cell co-staining. 4T1 cells were seeded in 35 mm plates and cultured for 24 hours. The cells were incubated with **PPSe** (0.25 and 0.5 μM) for 6 hours and then treated with or without irradiation (660 nm, 20 mW/cm^2, 10 min). The cell groups with or without irradiation

DOI: 10.55415/deep-2023-0016.v1

were used as controls. After 12 hours incubation, the cells were firstly washed with phosphate buffer solution and then co-stained with calcein AM/ PI for 30 min at 37 °C in the dark. Finally, all the groups of cells were imaged with a Confocal Laser Scanning Microscope.

2.8 Apoptosis assays

Cell apoptosis was analyzed by the Annexin V-FITC and PI apoptosis detection kit (Beyotime Biotechnology, Shanghai, China). 4T1 cells were cultured in 6-well Corning plates and incubated with **PPSe** (0.25 and 0.5 μM) at 37 °C for 6 h, and then treated with or without irradiation (660 nm, 20 mW/cm^2, 10 min). Incubating for 24 h after irradiation, 4T1 cells were collected and stained with Annexin V-FITC and PI at room temperature for 30 min to analyze cell apoptosis. Cell apoptosis was detected by flow cytometry (Beckman, USA), and the percentage of apoptotic cells were analyzed by FlowJo.

2.9 DNA damage, apoptosis and pyroptosis experiment (Western Blotting)

4T1 cells were seeded in 6-well Corning plates at a density of 2 × 10^5 cells/ well and incubated for 24 h. Then the cells were incubated with **PPSe** (0.25 μM) for 6 h and irradiated with 660 nm LED lamp (20 mW/cm^2, 10 min). Cells were collected after incubating for 24 h and then lysed by RIPA lysis solution (Beyotime Biotechnology, Shanghai, China) with the addition of protease/phosphatase inhibitors for 30 min in ice. After calibrating the concentration of protein, equal amounts of protein were added into SDS-PAGE gels electrophoresis and transferred to nitrocellulose (NC)

DOI: 10.55415/deep-2023-0016.v1

filter membranes. Primary antibodies were mouse monoclonal Caspase-3, γ-H2A.X, and β-actin antibodies. Anti-mouse IgG HRP-conjugated antibody was used as secondary antibodies. An ECL detection system was used to visualize the specific protein bands. The target protein levels were semi-quantitatively analyzed by Image J software.

2.10 Statistical analysis

The statistical analysis between groups was performed based on one-way analysis of variance (ANOVA) and student's t-test by GraphPad Prism 9.0.7. software. The results were expressed as mean ± standard deviation (SD). A p value < 0.05 was considered statistically significant (* $p < 0.05$, ** $p < 0.01$, *** $p < 0.001$).

3. RESULTS AND DISCUSSION

The photosensitizer **PPSe** was synthesized through redox-neutral annulation between readily accessible 3,3'-diselanediylbis (N, N-dimethyl-4-nitrosoaniline) and 4-((quinolin-8-ylamino) methyl) benzoic acid, as shown in Scheme S1.

The optical properties of **PPSe** were firstly analyzed by using UV-vis absorption and fluorescence spectra. As displayed in Figure 1b, the maximum absorption of **PPSe** centered at ~ 660 nm. Upon 660 nm light excitation, **PPSe** exhibited NIR-I emission with a maximum peak at ~ 690 nm.

The ROS generation capacity of **PPSe** was then evaluated since it represents the photodynamic efficacy of a photosensitizer. To determine whether **PPSe** could generate $^1O_2$, 1, 3-diphenylisobenzo-furan (DPBF) was used as the $^1O_2$ capture probe

DOI: 10.55415/deep-2023-0016.v1

and methylene blue (Φ_Δ = 0.52 in ethanol) was used as a reference (Figure 1c, d and Figure S1). As the irradiation time increases, the absorbance of the DPBF/**PPSe** EtOH solution decreased under 660 nm light irradiation (2 mW/cm^2). And the singlet oxygen quantum yield of **PPSe** in EtOH was determined to be 0.62, indicating that **PPSe** has strong singlet oxygen generation efficiency. To characterize the superoxide anion radical generation ability of **PPSe** in the aqueous solution upon irradiation, dihydrorhodamine 123 (DHR123) probe was used as the superoxide anion radical ($O_2^{\bullet-}$) indicator. There is no obvious fluorescence change in the DHR123 alone group under irradiation (660 nm, 10 mW/cm^2), but remarkable fluorescence enhancement of the **PPSe** (5 μM) and DHR123 (5 μM) group was observed, indicating the $O_2^{\bullet-}$ production (Figure 1e, 1f). Taken together, **PPSe** could efficiently produce ROS through both the electron and energy transfer processes. Thus, **PPSe** is a type I/II combined photosensitizer.

In order to investigate the cellular uptake efficiency of **PPSe**, flow cytometry was used to monitor the changes of fluorescence intensity in living cells. 4T1 cells were treated with **PPSe** (5 μM) in different time points (30 min, 1 h, 3 h, 6 h and 9 h). As shown in Figure 2a and 2b, right shift of the chromatogram represents increased fluorescent intensity which can indicate increased cellular uptake. It was observed that the cellular uptake of **PPSe** displayed a gradual increase over time, and saturated around 6 h. Overall, the cellular uptake experiment showed that **PPSe** could be efficiently taken up by breast cancer cells.

DOI: 10.55415/deep-2023-0016.v1

Since **PPSe** has exhibited the PDT potential by generating $^1O_2$ and $O_2^{\bullet-}$ as discussed above, the intracellular ROS produced by **PPSe** in living cells were further measured using 2′,7′-dichlorofluorescin diacetate (DCFH-DA) as a fluorescent probe. The breast cancer 4T1 cells were treated with **PPSe** (0.25 μM) for 6 hours, followed by incubating with the probe DCFH-DA (10 μM) for 30 min. As shown in Figure 2c and 2d, there were no obvious differences in the PBS groups with or without irradiation. The intracellular ROS level in the **PPSe** treated cells was found negligible in dark, but significantly increased upon 660 nm irradiation (20 mW/cm^2, 10 min). The results indicated that **PPSe** could efficiently induce ROS generation under light irradiation and might have potent phototoxicity.

To assess the photodynamic effect of **PPSe** against breast cancer cells, the cytotoxicity of **PPSe** against 4T1 cells was investigated using the Cell Counting Kit-8 (CCK-8) assay. As depicted in Figure 3a, the cell viabilities of 4T1 cells incubated with different concentrations of **PPSe** and exposed to different light doses (660 nm, 20 mW/cm^2, 4 J/cm^2, 8 J/cm^2 and 12 J/cm^2) were evaluated. The results indicated that the phototoxicity of **PPSe** increased in a dose-dependent manner within the investigated light dose ranges, and **PPSe** exhibited the best photodynamic efficacy under the irradiation of 12 J/cm^2 (20 mW/cm^2, 10 min). Notably, **PPSe** exhibited excellent cytotoxicity against 4T1 cell lines with an IC_{50} value of 170.2 ± 9.6 nM upon 660 nm light irradiation (12 J/cm^2), as shown in Figure 3b. Furthermore, the photodynamic effect of **PPSe** under hypoxia was also investigated. Owing to **PPSe** mainly generated $^1O_2$ following a type-II pathway, **PPSe** exhibited poor

DOI: 10.55415/deep-2023-0016.v1

phototherapeutic efficacy without a dose-dependent fashion under the condition of 1% O_2 (Figure S3). It is noteworthy that **PPSe** exhibited no significant dark toxicity within the tested concentrations, which indicated that **PPSe** have an excellent phototherapeutic index (> 58) against 4T1 cells.

To visually confirm the cytotoxicity of **PPSe**, the photodynamic effect of **PPSe** toward cancer cells was further evaluated by the live/dead cell co-staining assay using propidium iodide (PI) and calcein-AM. Calcein-AM stains live cells to emit green fluorescence, whereas PI stains dead cells to emit red fluorescence. As shown in Figure 3c, almost no cells were dead in the PBS control groups or the groups treated with **PPSe** (0.25 and 0.5 μM) without light irradiation, in which a large percentage of cells were stained green by calcein-AM. By contrast, the cancer cells treated with **PPSe** were significantly killed in a concentration-dependent manner upon light irradiation. As seen in Figure 3c, nearly half of the 4T1 cells were killed when incubated with 0.25 μM **PPSe** plus 660 nm light irradiation (20 mW/cm^2, 10 min). Meanwhile, significant red fluorescence was observed after treating 4T1 cells with 0.5 μM **PPSe** plus light irradiation, indicating almost all the cells were efficiently killed, which is correlated well with the cell viability assay.

To further evaluate the cytotoxicity of **PPSe** against human breast cancer cells, the cell viabilities of MDA-MB-231, MCF-7, MDA-MB-468 and MDA-MB-453 cells were also investigated via the CCK-8 assay. As shown in Figure 4 and Table S1, there were slight differences among the four breast cancer cell lines. The IC_{50} values of **PPSe** against the MDA-MB-231, MCF-7, MDA-MB-468 and MDA-MB-453 human

DOI: 10.55415/deep-2023-0016.v1

breast cancer cells lines under the condition of 660 nm light irradiation (20 mW/cm^2, 10 min) were 0.16 ± 0.010, 0.71 ± 0.061, 0.12 ± 0.014 and 0.29 ± 0.012 μM, respectively, which were similar with that of 4T1 cells. Meanwhile, the dark toxicity of **PPSe** was also investigated under the same experimental conditions except for light irradiation. It was shown that **PPSe** exhibited weak dark toxicity within the tested concentrations against the breast cancer cell lines. It should be noted that the phototherapeutic index of **PPSe** against MDA-MB-231 cells is quite excellent (>125).

Subsequently, the flow cytometry assays with Annexin V-FITC/PI staining were performed to evaluate the apoptotic effects of **PPSe** on 4T1 cells. As illustrated in Figure 5a and 5b, the percentage of apoptotic cells were significantly increased in the **PPSe** plus irradiation (660 nm, 20 mW/cm^2, 10 min) groups compared with the **PPSe** alone groups. The cell apoptotic rates in the **PPSe** (0.25 μM) alone group and the **PPSe** (0.25 μM) plus irradiation group were 2.31% and 17.32%, respectively. When the 4T1 cells were incubated with 0.5 μM **PPSe** plus irradiation, the cell apoptotic rate was significantly increased to 32.51%. By contrast, there was no significant change in the cell apoptosis rate of the PBS groups regardless of irradiation or not. Taken together, **PPSe** could efficiently induce 4T1 cells apoptosis under light irradiation and the percentage of apoptotic cells increased when increasing the concentration of **PPSe**, which is well consistent with the cytotoxicity of **PPSe**.

To further investigate the mechanism of cell death induced by **PPSe** under light irradiation, we performed western blot assays to monitor DNA damage and apoptosis

DOI: 10.55415/deep-2023-0016.v1

in 4T1 cells. As shown in Figure 5c, the expression of cleaved-caspase-3 and the γ-H2A.X increased significantly in the **PPSe** (0.5 μM) plus light irradiation (660 nm, 20 mW/cm^2, 10 min) group, but not in the **PPSe** alone (0.5 μM) and the PBS control groups. These results indicated that the combination of **PPSe** and light irradiation could lead to efficient DNA damage and induce apoptosis.

4. CONCLUSIONS

To sum up, we have described the discovery and characterization of a new NIR-I photosensitizer **PPSe** that can efficiently generate ROS via a type I and type II combined pathway in the presence of light. **PPSe** exhibited potent phototoxicity against five breast cancer cell lines. It is noteworthy that the phototherapeutic index of **PPSe** against MDA-MB-231 cells is very excellent (>125). Cell death mechanism studies indicated that **PPSe** could induce DNA damage and cell apoptosis in the presence of light. We hope that **PPSe** will find more applications in photodynamic therapy.

ACKNOWLEDGEMENTS

The authors acknowledge the National Natural Science Foundation of China (No. 82003589), the Taishan Scholars Program at Shandong Province (No.tsqn 201909036) and the Qilu Scholar Program at Shandong University for financial support. The authors also acknowledge the Natural Science Foundation of Shandong Province (No. ZR2022QC058) and the Guangdong Basic and Applied Basic Research Foundation (2022A1515110292).

DOI: 10.55415/deep-2023-0016.v1

CONFLICTS OF INTEREST

The authors declare no competing financial interest.

REFERENCES

[1] S Becker: **A historic and scientific review of breast cancer: The next global healthcare challenge.** *Int J Gynaecol Obstet* 2015,131 Suppl 1:S36-9

[2] S J Henley, C C Thomas, D R Lewis, E M Ward, F Islami, M Wu, H K Weir, S Scott, R L Sherman, J Ma, B A Kohler, K Cronin, A Jemal, V B Benard, L C Richardson: **Annual report to the nation on the status of cancer, part II: Progress toward Healthy People 2020 objectives for 4 common cancers.** *Cancer* 2020,126:2250-2266

[3] H Sung, J Ferlay, R L Siegel, M Laversanne, I Soerjomataram, A Jemal, F Bray: **Global Cancer Statistics 2020: GLOBOCAN Estimates of Incidence and Mortality Worldwide for 36 Cancers in 185 Countries.** *CA Cancer J Clin* 2021,71:209-249

[4] J Choi, W H Jung, J S Koo: **Clinicopathologic features of molecular subtypes of triple negative breast cancer based on immunohistochemical markers.** *Histol Histopathol* 2012,27:1481-93

[5] C Kim, R Gao, E Sei, R Brandt, J Hartman, T Hatschek, N Crosetto, T Foukakis, N E Navin: **Chemoresistance Evolution in Triple-Negative Breast Cancer Delineated by Single-Cell Sequencing.** *Cell* 2018,173:879-893 e13

[6] C A Parise, V Caggiano: **Breast Cancer Survival Defined by the ER/PR/HER2 Subtypes and a Surrogate Classification according to Tumor Grade and Immunohistochemical Biomarkers.** *J Cancer Epidemiol* 2014,2014:469251

[7] F C Geyer, F Pareja, B Weigelt, E Rakha, I O Ellis, S J Schnitt, J S Reis-Filho: **The Spectrum of Triple-Negative Breast Disease: High- and Low-Grade Lesions.** *Am J Pathol* 2017,187:2139-2151

[8] C M Perou: **Molecular stratification of triple-negative breast cancers.** *Oncologist* 2011,16 Suppl 1:61-70

[9] M Czarnecka-Czapczynska, D Aebisher, P Oles, B Sosna, M Krupka-Olek, K Dynarowicz, W Latos, G Cieslar, A Kawczyk-Krupka: **The role of photodynamic therapy in breast cancer - A review of in vitro research.** *Biomed Pharmacother* 2021,144:112342

DOI: 10.55415/deep-2023-0016.v1

[10] X Li, J F Lovell, J Yoon, X Chen: **Clinical development and potential of photothermal and photodynamic therapies for cancer.** *Nat Rev Clin Oncol* 2020,17:657-674

[11] S Z Zeping Gao, Ken-ichiro Kamei, and Chutong Tian: **Recent progress in cancer therapy based on the combination of ferroptosis with photodynamic therapy.** *Acta Materia Medica* 2022,1:411-426

[12] T C Pham, V N Nguyen, Y Choi, S Lee, J Yoon: **Recent Strategies to Develop Innovative Photosensitizers for Enhanced Photodynamic Therapy.** *Chem Rev* 2021,121:13454-13619

[13] D Chen, Q Xu, W Wang, J Shao, W Huang, X Dong: **Type I Photosensitizers Revitalizing Photodynamic Oncotherapy.** *Small* 2021,17:e2006742

[14] Y Wan, L H Fu, C Li, J Lin, P Huang: **Conquering the Hypoxia Limitation for Photodynamic Therapy.** *Adv Mater* 2021,33:e2103978

[15] J F Lovell, T W Liu, J Chen, G Zheng: **Activatable photosensitizers for imaging and therapy.** *Chem Rev* 2010,110:2839-57

DOI: 10.55415/deep-2023-0016.v1

Graphic abstract

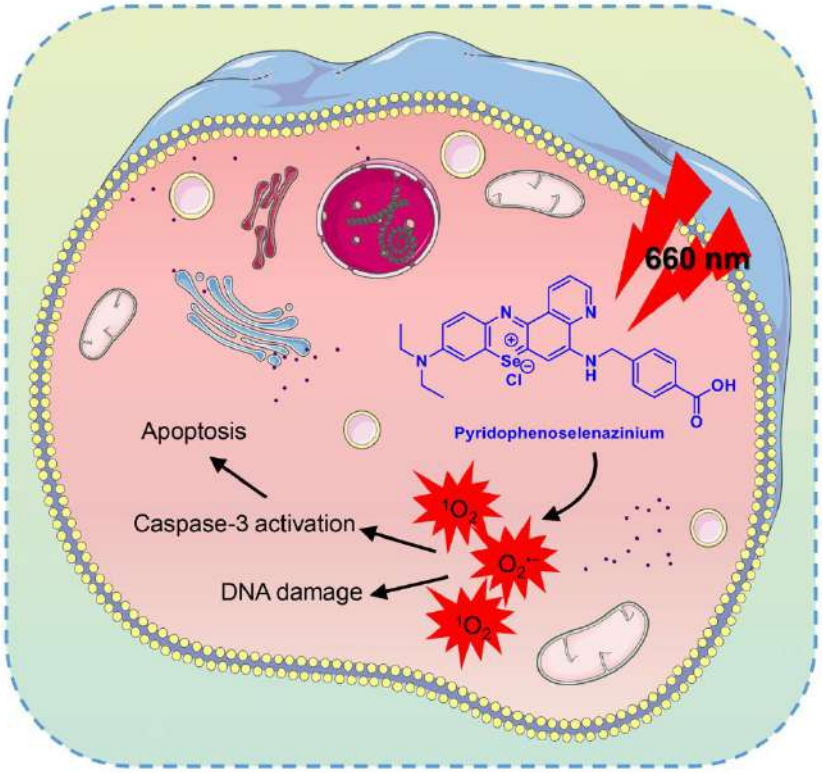

DOI: 10.55415/deep-2023-0016.v1

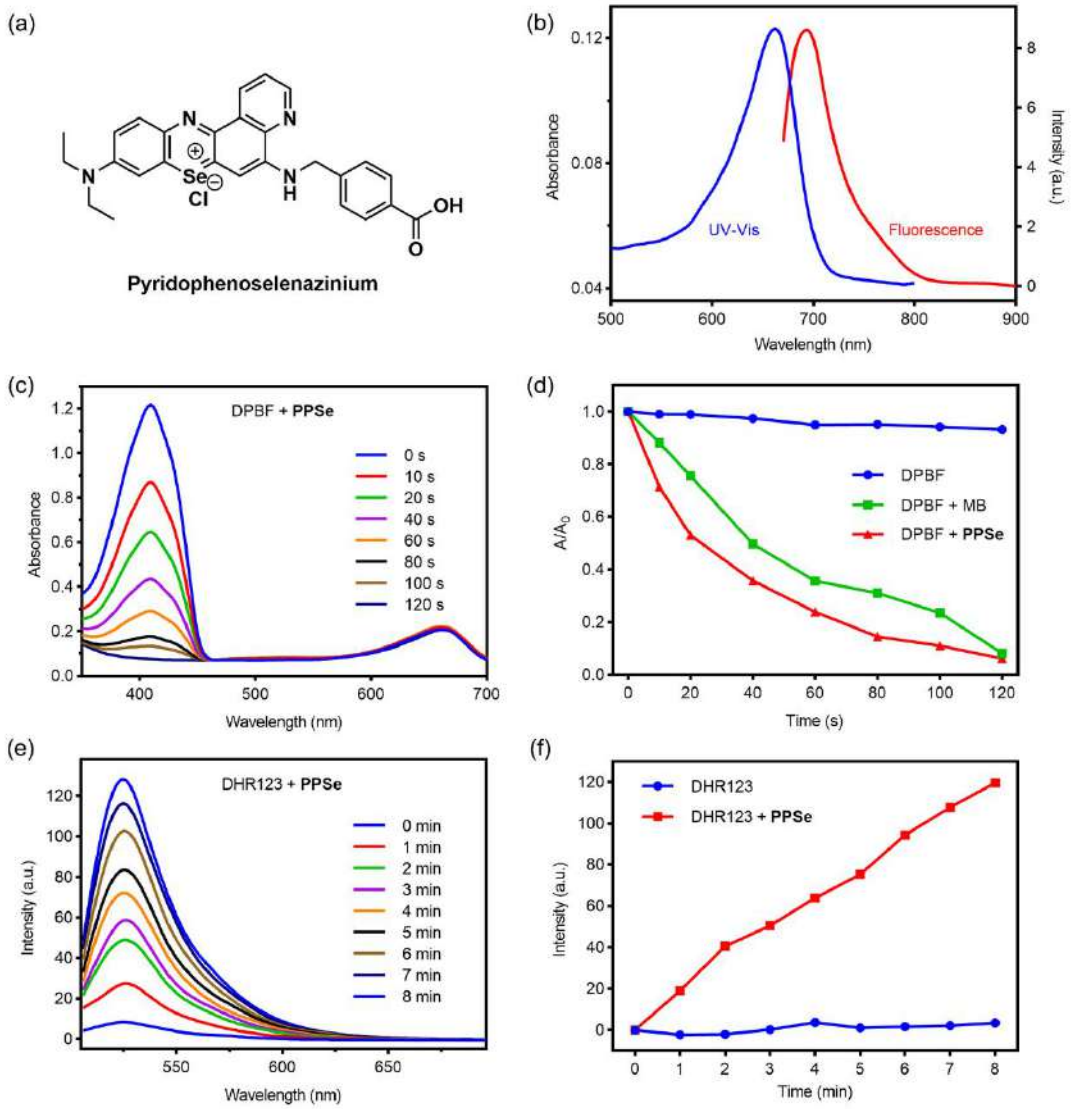

Figure 1. (a) The structure of the photosensitizer **PPSe**. (b) UV-vis and fluorescence spectra of **PPSe** in ethanol. (c-d) Absorption changes of the DPBF/ **PPSe** under 660 nm LED light irradiation (2 mW/cm^2) in EtOH solution. (e) $O_2^{\bullet-}$ detection using the DHR123 (5 μM) assay for **PPSe** (5 μM) in aqueous solution upon irradiation (660 nm, 10 mW/cm^2). (f) Fluorescence response of DHR123 for **PPSe** (5 μM) and DHR123 (5 μM) in aqueous solution.

DOI: 10.55415/deep-2023-0016.v1

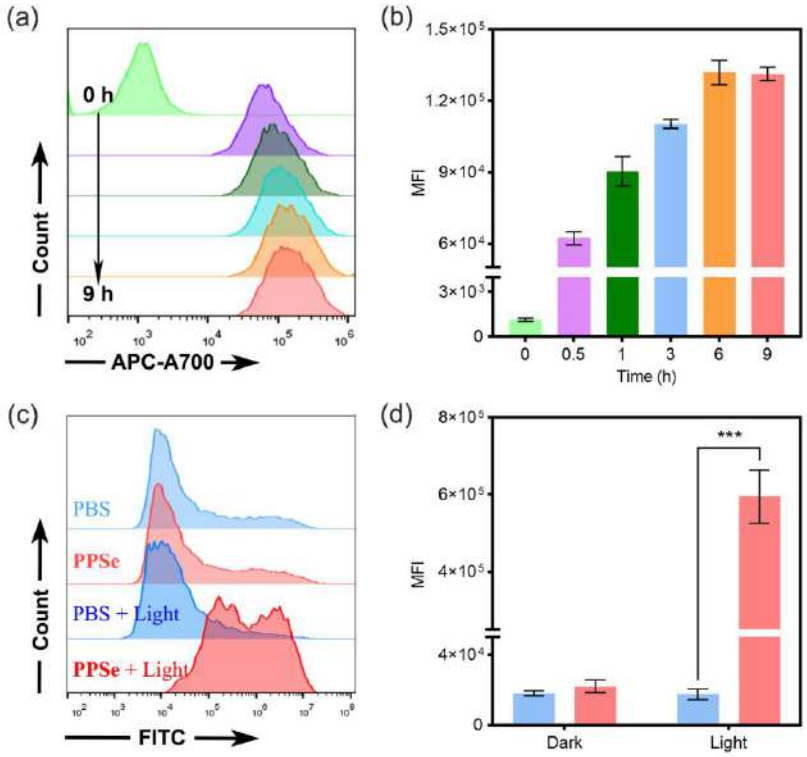

Figure 2. (a-b) Flow cytometry analysis and the curve of median fluorescence intensity of cellular uptake of **PPSe** (5 μM) after incubation for different time period. (c-d) Flow cytometry analysis and the curve of median fluorescence intensity of ROS generation in 4T1 cells treated with **PPSe** (0.25 μM) with or without light irradiation (660 nm, 12 J/cm^2).

DOI: 10.55415/deep-2023-0016.v1

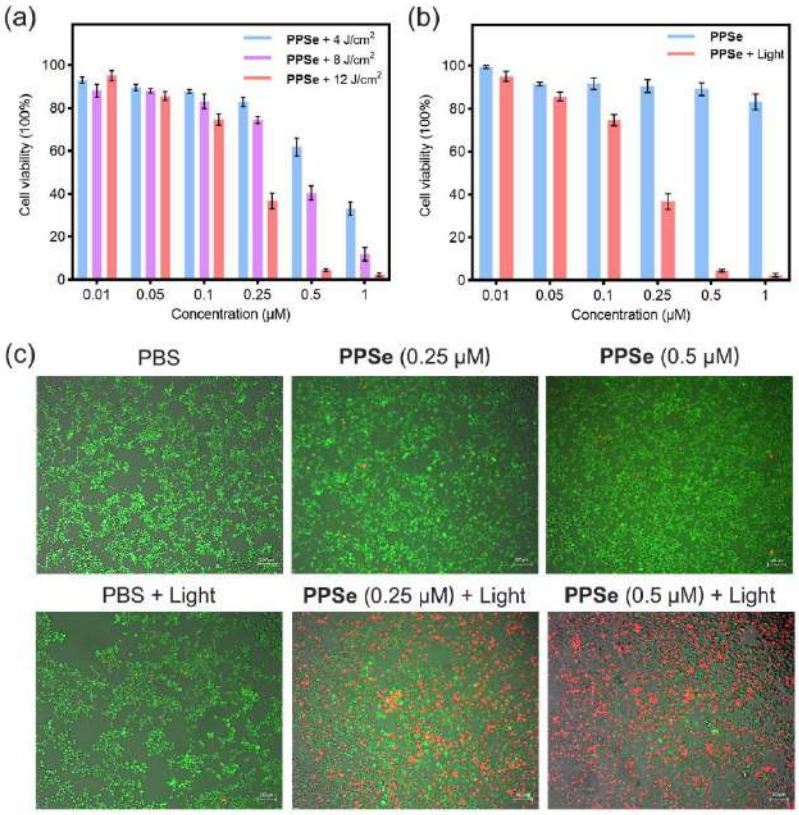

Figure 3. (a) Cell viabilities of 4T1 cells incubated with varied concentrations of **PPSe** after exposure to different light dose (660 nm). (b) Cell viabilities of 4T1 cells incubated with varied concentrations of **PPSe** with or without irradition (660 nm, 12 J/cm^2). (c) Fluorescence images of Calcein-AM and PI costained 4T1 cells treated with **PPSe** with or without irradition, the irradiation is 660 nm, 12 J/cm^2. Scale bar: 100 μm.

DOI: 10.55415/deep-2023-0016.v1

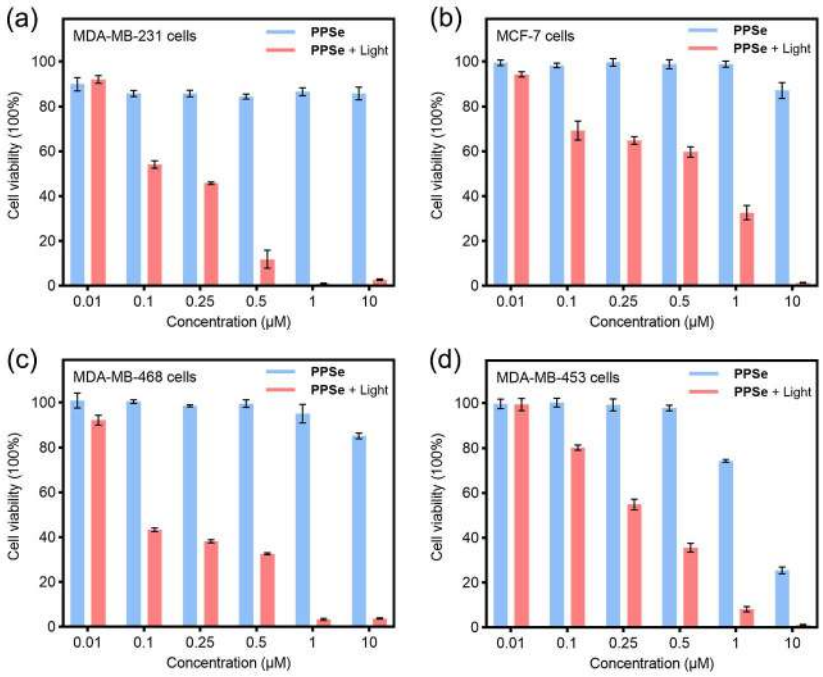

Figure 4. MDA-MB-231 (a) MCF-7 (b) MDA-MB-468 (c) and MDA-MB-453 (d) cell viabilities after incubation with varied concentrations of **PPSe** with or without irradition (660 nm, 12 J/cm^2).

DOI: 10.55415/deep-2023-0016.v1

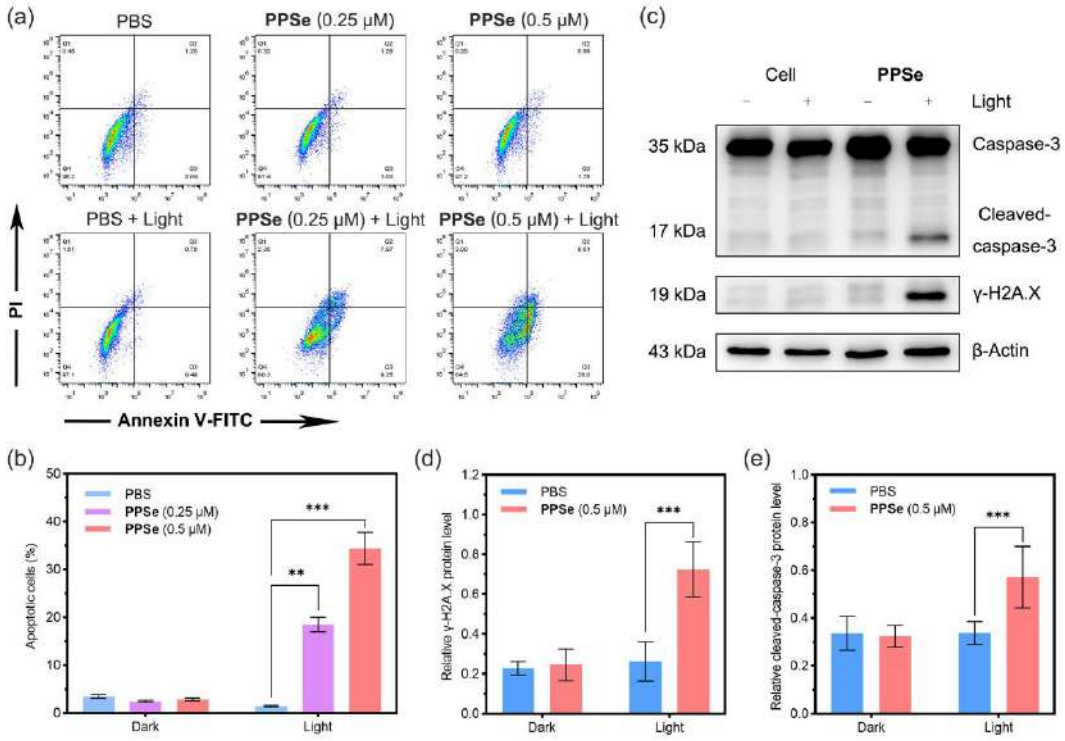

Figure 5. (a-b) Effects of **PPSe** on cell apoptosis in 4T1 cells. (c) Western blot assay of DNA damage-relevant protein γ-H2A.X and apoptosis-relevant protein cleaved caspase-3 protein in 4T1 cells, β-actin utilized as an internal loading control. (d-e) Quantitative protein expression of cleaved caspase-3 and γ-H2A.X. All values are means ± SD.